Effect of calcium format on the hydration characteristics of Supersulfated cement

Article Type: Research Article Authors: H.H.M. Darweesh

Article publication history:

Article Received on: Apr 29, 2025 Article Accepted on: June 07, 2025 Article Published on: Sep 10, 2025

Article review details:

1st Review By. Dr. Shamim Ansari 2nd Review By. Dr. Amit Soni

Final Recommendation By: Prof: Nitesh Pathak

Affiliation:

Department of Refractories, Ceramics and Building Materials, National Research Centre, Cairo, Egypt

ISSN: 2581-7760

Corresponding Email:

hassandarweesh2000@yahoo.com

Abstract

Supersulfated cement (SSC) was prepared from 85 wt. % granulated blast furnace slag (GbfS), 10 wt. gypsum (GY) and 5 wt. % Portland cement clinker (PCC). The main objective of this study is to improve the early strength of SSC with the addition of calcium format activator (CF). Different dosages of 0, 0.5, 1, 1.5, 2, 2.5, 3 and 3.5 wt. % CF were added to the SSC. The results showed that the water of consistency and setting times were increased as the content of CF increased. The total porosity and water absorption were slightly decreased with the increase of CF content, whereas the bulk density was improved an enhanced. The flexural and compressive strength also improved and gradually increased with CF addition. The combined water contents improved wand enhanced with the gradual replacement of CF. This was continued up till 3 wt. % CF, but with any further increase more than that, all of the hydration characteristics were diminished. The reacted or combined slag or sulfate increased with curing time. So, the CF would significantly improve, increase and also accelerate the early and later hydration characteristics of the SSC, and the dosage of 3 wt. % CF was the more pronounced effect compared with that of the control, i.e. the optimum CF dosage was 3 wt. %.

Keywords: upersulfated cement, Calcium format, Consistency and setting time, Absorption, Porosity, Density, Flexural strength, Compressive strength

Introduction

Carbon dioxide emission (CO₂) during cement manufacturing is a significant anthropogenic contributor to global warming, where 7-37 % of global anthropogenic CO₂ emissions and 2-3% of energy consumption occurred [1-3]. Global warming may lead to substantial economic losses and human casualties [3, 4]. Production of Portland cement (PC) worldwide has been recently reached to 4.6 billion tones, and it is expected to be 6 billion tones by 2050 [5,6]. Production of PC would consume huge amounts of resources and energy and it

emits a great amount of CO₂ [7, 8]. To reduce the emission of CO₂, low-carbon cement has been focused, where supersulphated cement (SSC) is a typical low-carbon cement, consisting of less than 5 wt. % of an alkaline activator, as Portland cement clinker (PCC), more than 80 wt. % granulated blast furnace slag (GbfS) and 10-15 wt. % gypsum [9, 10], which has recently received much attention. The GbfS is an industrial byproduct which is coming from the manufacture of the pig iron in the blast furnace. It is formed during the firing of the earthy constituents of the iron ore with the limestone flux. The essential components of GbfS are the same as those of Portland cement clinker, namely lime, silica, alumina, but with slighter lower percentages. The quality of GbfS could be determined from the following relation:-

$$M = CaO + MgO + Al_2O_3 / SiO_2 + MnO \rightarrow 1$$
 (1)

The hydraulic quality of GbfS depends on its contents of Al₂O₃ and CaO. The reactivity of GbfS was due to a stable protective film that consisting of a Si-O network. However, the strength development of SSC is quite slow due to the lower alkaline activator content [11], which is one of its main short comings. Wang et al. [12] found that increasing the fineness of slag would promote the strength development. Slag of higher Al₂O₃ content (>13 %) displayed a higher degree of hydration [13]. Calcium formate (CF) is a commonly used earlystrength agent of PC and can improve the early strength of cement mortars and concrete [14, 15], although it has a little beneficial effect on the long-term strength. However, CF has a beneficial effect on both the early and long-term strength of high-volume slag cementitious systems [16]. CF could promote the precipitation of AFt in the slag-fly ash cementitious system, accelerating the hydration of silicate in SCMs [17]. In addition, CF could improve the dissolution of the slag of a CaO-activated slag system, by increasing the calcium and aluminate ions, producing more hydration products such as C-S-H and C₂AH₈ [18]. Dalconi [19] also found that formate ions could react with calcium aluminate to produce formate-based hydration products similar to calcium aluminate hydrates. In fact, SSC is also a typical highvolume slag system, and CF could have the potential to efficiently improve the performance of the SSC. In this study, different dosages of CF (1, 1.5, 2, 2.5, 3 wt. %) were added to the SSC. The compressive strength, hydration heat flow, hydration products, and hydration degree of the slag were obtained to find the role of the CF on the mechanical performance and hydration mechanism of the SSC.

Experimental

Raw materials

The main raw materials of the supersulfated cement (SSC) are granulated blast furnace slag (GbfS), Portland cement clinker (PCC), gypsum (GY) and calcium format (CF). GbfS, PCC and GY were delivered from Sakkara cement factory, Giza, Egypt. The CF was obtained from El-Gommhoria Company for chemicals, Ramses street, Egypt. The chemical oxide compositions of the raw materials are presented in Table 1. The particle size distributions of the GbfS, PCC and GY are shown in Fig. 1, where the GbfS is the most fineness, whereas the GY is the lowest. Table 2 shows the constitutions of the used samples of raw materials forming supersulfated cement.

Table 1: Chemical composition of GbfS and PCC, wt. %.

Oxides Materials	SiO ₂	Al_2O_3	Fe ₂ O ₃	CaO	MgO	Na ₂ O	K ₂ O	SO_3	LOI
PCC	20.13	3.86	2.78	63.87	1.83	0.31	1.07	3.11	4.12
GbfS	41.79	18.69	2.59	29.31	10.13	0.45	1.31	2.74	1.36

Table 2: Constitution of the supersulfated cement, wt. %.

	Mixes Materials	K0	K1	K2	K3	K4	K5	K6
GbfS		90	89.5	89	88.5	88	87.5	87
PCK		10	10	10	10	10	10	10
CF		0	0.5	1.0	1.5	2.0	2.5	3.0

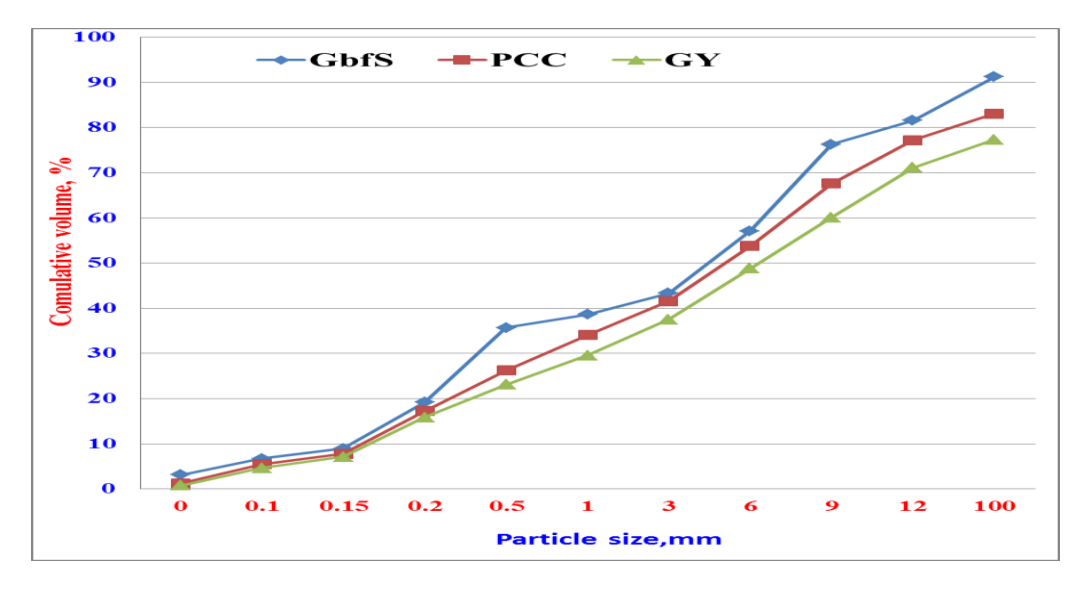


Fig. 1-Particle size distribution of the raw materials

Preparation and methods

During the preparation of supersulfated cement, different dosages of CF (0, 0.5, 1, 1,5, 2, 2,5, 3, 3.5 wt. %) were added to the cement mixtures at the expense of PCC. These mixes were denoted as F0, F1, F2, F3, F4, F5, F6 and F7, respectively. The CF was first dissolved into the mixing water, and then the solution was poured into the prepared SSC in a suitable mixer. The blending process of the various cement blends was done in a porcelain ball mill containing 2-4 balls for two hours to assure the complete homogeneity of all cement blends.

The cement pastes were then cast using the predetermined water of consistency, moulded into one inch cubic stainless steel molds of dimensions 2.5 x 2.5 x 2.5 cm³ using about 500 g

cement mix, vibrated manually for three minutes and then on a mechanical vibrator for another three minutes. The surface of the molds was smoothed using a suitable spatula. Thereafter, the molds were kept in a humidity chamber for 24 hours under 95±1 RH and room temperature of 23 °C, demolded in the next day and soon immersed in water till the time of testing at 1, 3, 7, 28 and 90 days.

Physical properties

Standard water of consistency (or mixing water) as well as setting times (initial and final) of the prepared cement pastes were directly determined using needles penetration resistance of Vicat Apparatus [20-22].

WC,
$$\% = A / C \times 100$$
 (2)

Where, A is the amount of water taken to produce a suitable paste, C is the amount of cement (300 g). The initial setting time (IST) is the time taken to reach the initial set, while the final setting time (FST) is the time taken to reach the final set of the paste [22].

During mixing, the right w/c-ratio was poured into the cement portion inside the mixer and then run the mixer for about 5 minutes at an average speed of 10 rpm in order to have a perfect homogenous mixture. The water absorption, bulk density and apparent porosity[23-27] of the hardened cement pastes were calculated from the following equations:

$$WA,\% = (W1-W2) / (W3) X 100$$
 (3)

B. D,
$$(g/cm^3) = W_1 / (W_1 - W_2) \times 1$$
 (4)

A. P.,
$$\% = (W_1 - W_3) / (W_1 - W_2) \times 100$$
 (5)

Where, B.D, A.P, W₁, W₂ and W₃ are the bulk density, apparent porosity, saturated, suspended and dry weights, respectively.

Mechanical properties

Flexural strength (FS) was calculated following ASTM C348-21 [28]. The samples were marked at three points adjusting to place them on the correct point of contact (Fig. 2). FS was obtained from the following equation:-

$$FS = 3 (PL) / 2 (b) (d) / 10.2 MPa$$
 (6)

Where, L: load taken, P: bean or loading of rupture, b: width, d: thickness.

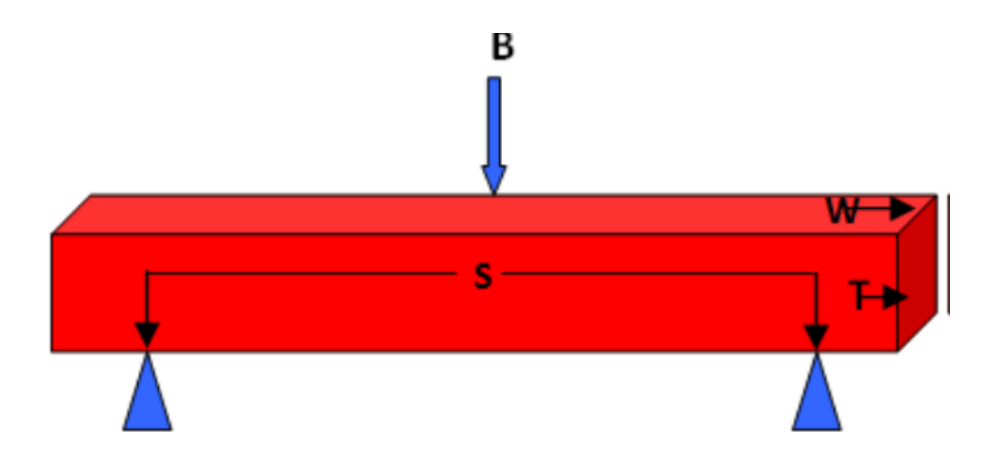


Fig. 2. Schematic diagram of bending strength, B: Beam or loading of rupture, S: Span, W: Width and T: Thickness.

The compressive strength (29) was measured by using a hydraulic testing machine of the Type LPM 600 M1 SEIDNER (Germany) having a full capacity of 600 KN and the loading was applied perpendicular to the direction of the upper surface of the cubes as follows:

$$Cs = L (KN) / Sa (cm2) KN/m2 x 102 (Kg/cm2)/10.2 (MPa)$$
(7)

Where, Cs: Compressive strength (MPa), L: load (KN), Sa: surface area (cm²).

Combined water content

The chemically-combined water content at each hydration age was also determined on the basis of ignition loss (25-27,30) as follows:

$$Wn, \% = W1 - W2 / W2 \times 100$$
 (8)

Where, Wn, W1 and W2 are combined water content, weight of sample before and after ignition, respectively. Also, the combined slag and sulfate were measured [31].

The phase compositions of some selected samples were investigated using infrared spectroscopy (IR) and scanning electron microscopy (SEM). The IR spectra were performed by Pye-Unicum SP-1100 in the range of 4000-400 cm⁻¹. The SEM images of the fractured surfaces, coated with a thin layer of gold, were obtained by JEOL-JXA-840 electron analyzer at accelerating voltage of 30 KV.

Results and Discussion

Water of consistency and setting time

The water of consistency and setting times (initial and final) of the various SSC cement pastes incorporating CF (F0-F7) is graphically represented in Fig. 3. The water of consistency of SSC pastes is sharply increased with the increase of CF content. This is mainly due to that both

GbfS and CF need a lot of water to produce a suitable paste. Furthermore, the alkali CF activator always requires more water to be reactive normally with the SSC cement [9,32,33]. Above 35 % water content, the workability had become unsuitable. So, the mixing water must not exceed up to 35 %. On the other side, the setting times also displayed the same trend, i.e. the setting times enhanced as the CF content increased [11,32,33].

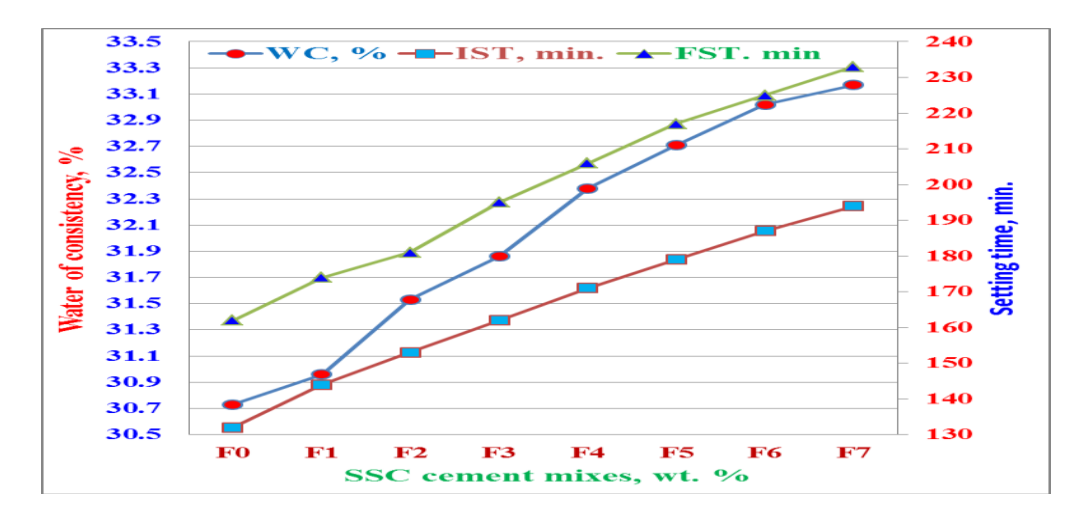


Fig. 3. Water of consistency and setting time of SSC cement pastes mixed with different ratios of CF activator.

Physical properties

Water absorption

Water absorption of the various SSC pastes containing CF (F0-F7) is graphically plotted as a function of curing times up to 90 days in Fig. 4. As CF activator content increased, the water absorption decreased, but only up till 3 %. Also, the occurrence of more compaction of the cement matrix with the incorporation of CF led to the shortened of water absorption. With any further increase in the CF content (F7), the water absorption increased and adversely affected, where it exhibited the highest values of water absorption. This may be due to that the higher content of CF activator could dissolve some silicate and/or alumino-silicate phases, which was generating an excess of more open pores [32,33]. Moreover, the high water of consistency helped more to increase the water absorption. In addition, by the excess of CF content > 3 wt. %, the water absorption increased. This is contributed to that the CF are more porous and also the high w/c ratio increased the water absorption [32-34].

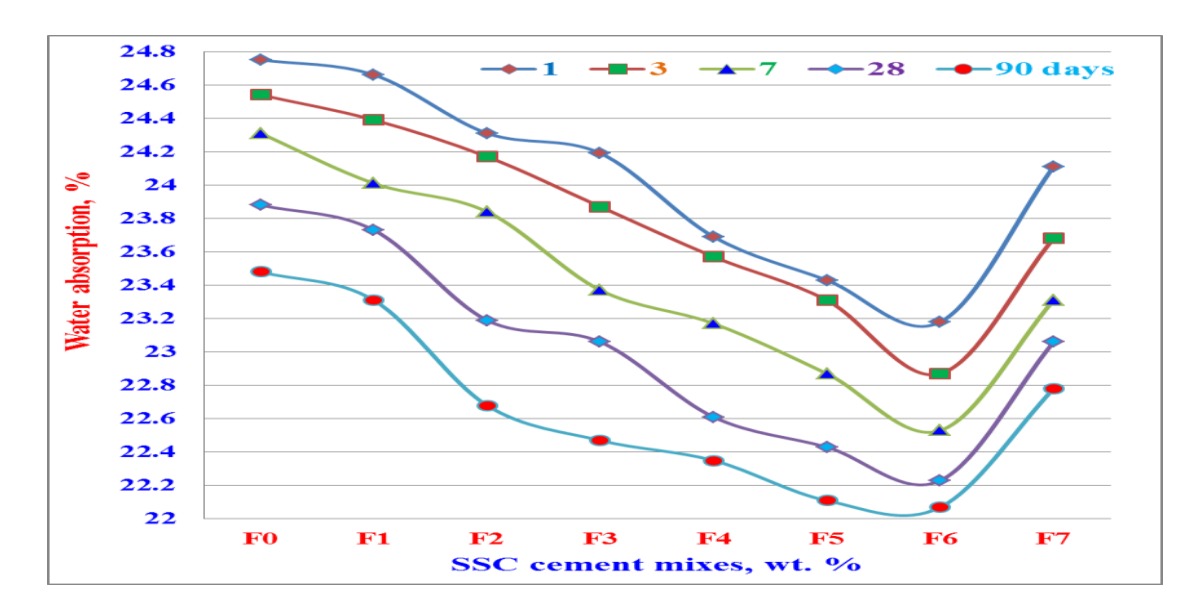


Fig. 4. Water absorption of SSC cement pastes mixes with different ratios of CF activator and hydrated up to 90 days

Bulk density

Figure 5 shows the bulk density of the various SSC pastes containing different ratios of CF (F0-F7) that is graphically drawn versus the curing times up to 90 days. Generally, the bulk density of the various SSC cements slightly increased at early ages of hydration, but only up to 3 wt. % (F1-F6), and then decreased with further CF increase (F7). The increase of bulk density is surely due to the decrease of water absorption and the good compaction of the cement matrix by the incorporation of CF [32-34]. The decrease of bulk density due to the incorporation of larger content of CF is mainly contributed to the creation of more open pore structure, where samples of higher CF content (F7) recorded the lowest values of bulk density. This may be due to that the higher content of CF activator could dissolve some silicate and/or alumino-silicate phases, which often created more open pores structure [33]. With any further increase of CF content > 3 wt. %, the bulk density declined, This is mainly contributed to that the higher CF content originated more porous matrix with the aid of higher w/c ratio [35,36].

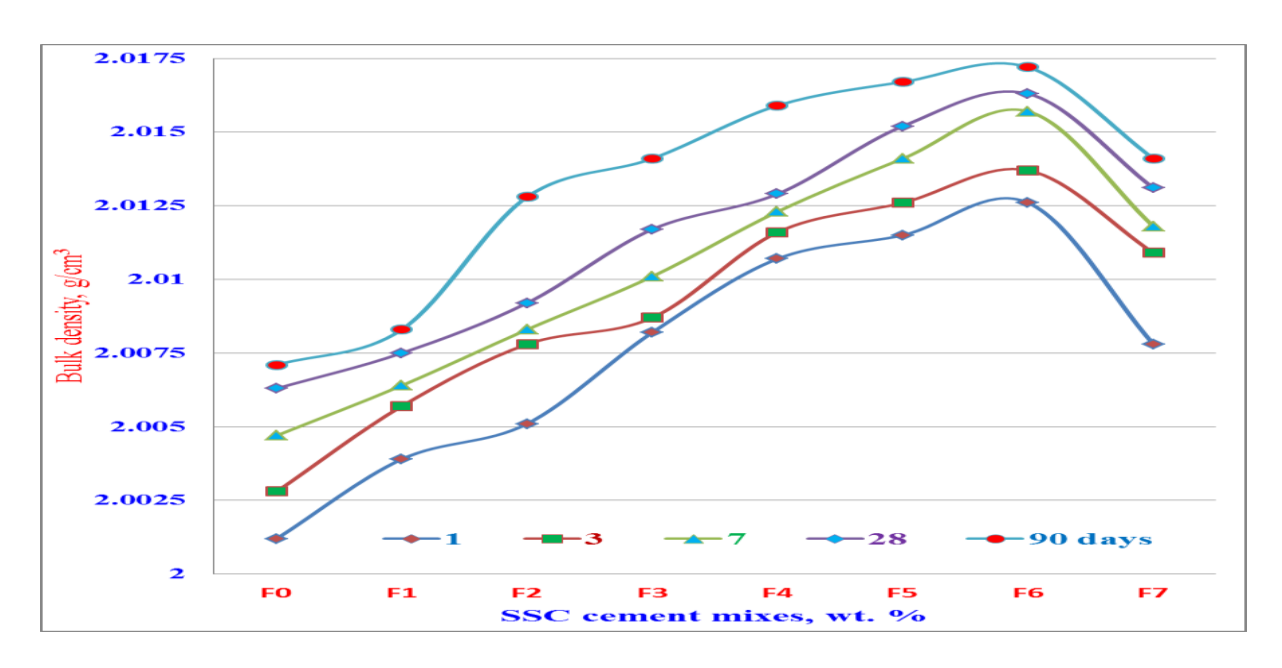


Fig. 5. Bulk density of SSC cement pastes mixes with different ratios of CF activator and hydrated up to 90 days.

Apparent porosity

The apparent porosity of the various SSC pastes containing different ratios of CF (F0-F7) is drawn versus curing times up to 90 days in Fig. 6. Generally, the apparent porosity of the various cements decreased as the curing time progressed up to 90 days. As the CF activator content increased, the apparent porosity decreased, but only up till 3 wt. % (F6). This is because the incorporation of CF could be made the total cement paste well compacted, which in turn reflected positively on the porosity, i.e. the porosity decreased or closed completely [34-36]. With any further increase of CF content > 3 wt. % (F7), the apparent porosity gradually increased, i.e. the higher CF activator content (F7) negatively affected and recorded the highest values of apparent porosity. This may be due to that the higher content of the CF activator could be dissolved some silicate and/or alumino-silicate phases, which in turn created more open pore structure, i.e. the high CF content originated more porous matrix with the help of the higher w/c ratio [32,33,37,38].

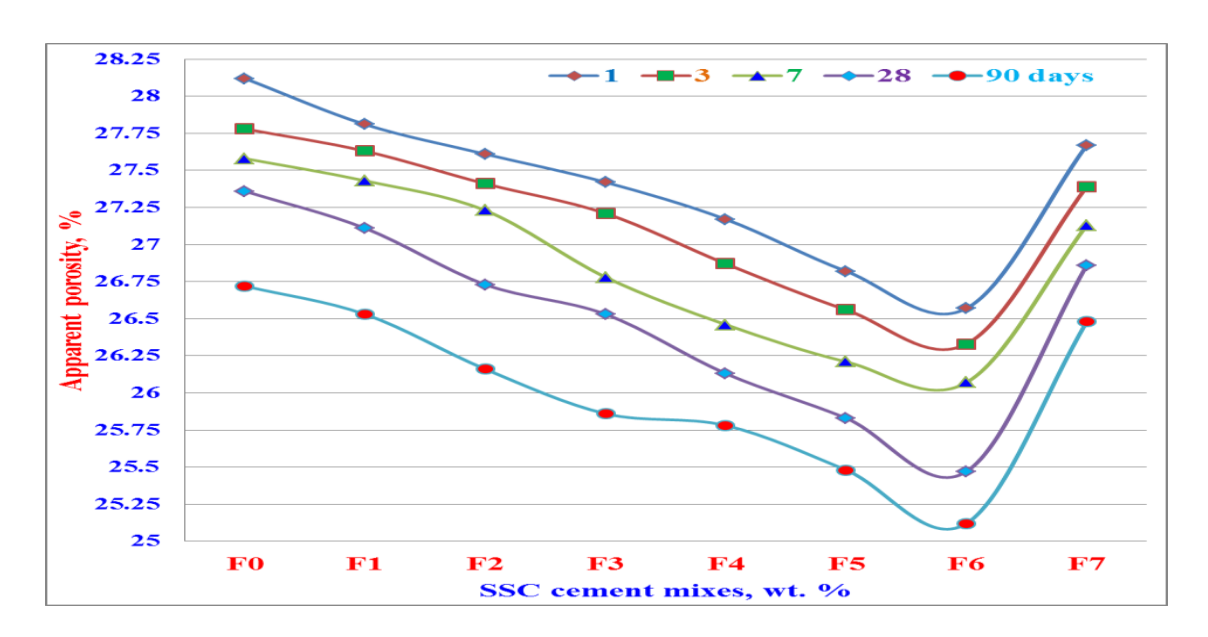


Fig. 6. Apparent porosity of SSC cement pastes mixes with different ratios of CF activator and hydrated up to 90 days.

Mechanical properties

Flexural strength

Figure 7 shows the results of flexural strength of the various SSC pastes (F0-F7) that drawn as a function of curing times up to 90 days. The flexural strength of the control SSC cement (F0) was increased as the curing time proceeded up to 90 days. The same trend was displayed by all SSC mixes blended with CF (F1-F7), but as the CF content enhanced, the flexural strength was enhanced too. This is mainly contributed to that the CF initiated the different phases of SSC [39,40], i.e. the CF was so improved and activated the hydration process. This in turn could be increased the rate of hydration of slag phases. At early ages of hydration (1-7 days), the flexural strength slightly increased, but then it hardly developed and highly increased at 28 days and also up to 90 days [41-43]. The SSC (F0) achieved the lowest flexural strength, whereas F7 exhibited the highest flexural strength at 90 days. Blending the SSC with CF > 3%, the flexural strength was sharply reduced. This is essentially attributed to that the higher alkaline activator content adversely affected the flexural strength. Consequently, the high content of CF > 3% must be avoided [42-44].

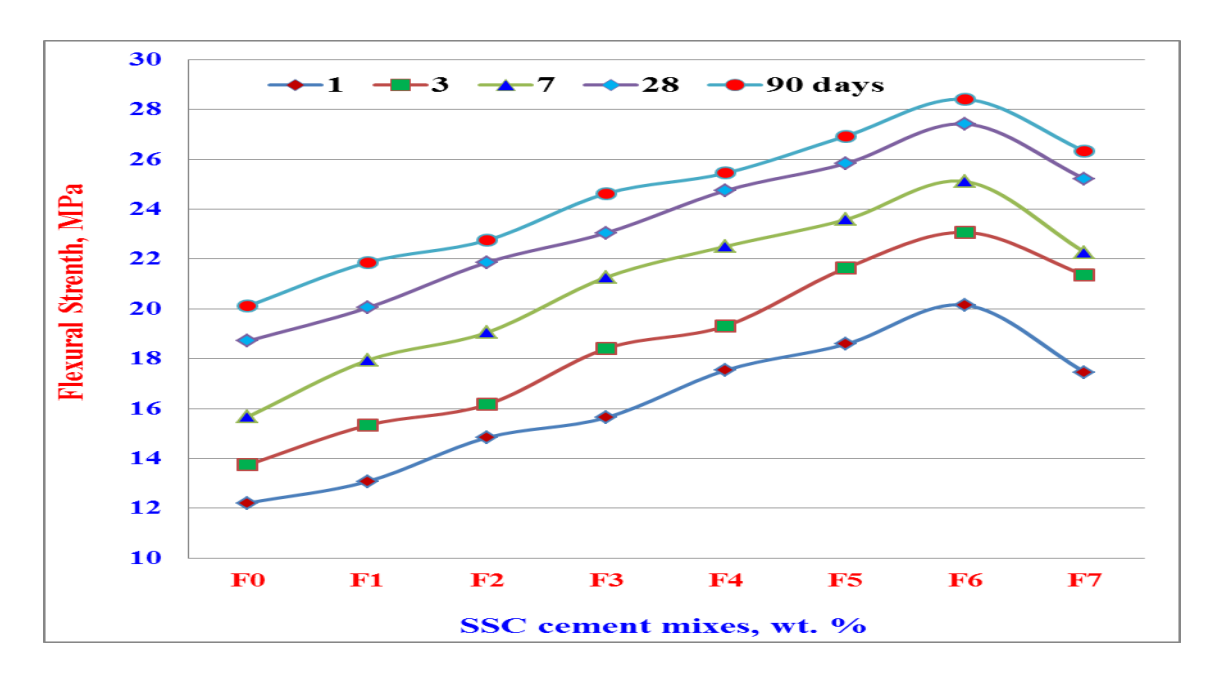


Fig. 7. Flexural strength of SSC cement pastes mixes with different ratios of CF activator and hydrated up to 90 days.

Compressive strength

The results of compressive strength are represented as a function of curing times in Fig. 8. As it is clear, the compressive strength of the control SSC cement (F0) was increased with curing time up to 90 days. The same trend was displayed by all SSC mixes blended with CF (F1-F6), but as the CF content increased, the compressive strength was increased too. This is mainly attributed to that the CF initiated and activated the phases of SSC or it may modify the hydration products [39,40], i.e. the CF was so improved the compressive strength that it could be accelerated the rate of hydration reactions of slag phases. At early ages of hydration (1-7 days), the compressive strength slightly increased, but then it hardly developed and sharply increased at 28 days and up to 90 days [17,41-43]. The SSC (F0) achieved the lowest compressive strength, whereas F6 recorded the highest compressive strength at 90 days. Blending the SSC with CF > 3%, the compressive strength was sharply diminished. This is essentially due to the higher alkaline activator content [44-47]. Consequently, the higher content of CF > 3 % must be prevented. Furthermore, the increase effect of CF activator is attributed to a more appropriate hydration environment, i.e. higher Ca²⁺ ions and lower pH-value. This often promotes the precipitation of C-A-S-H hydrates and inhibits the over rapid formation of ettringite (Aft) and reduces the crystal-gel ratio of the system [44-46].

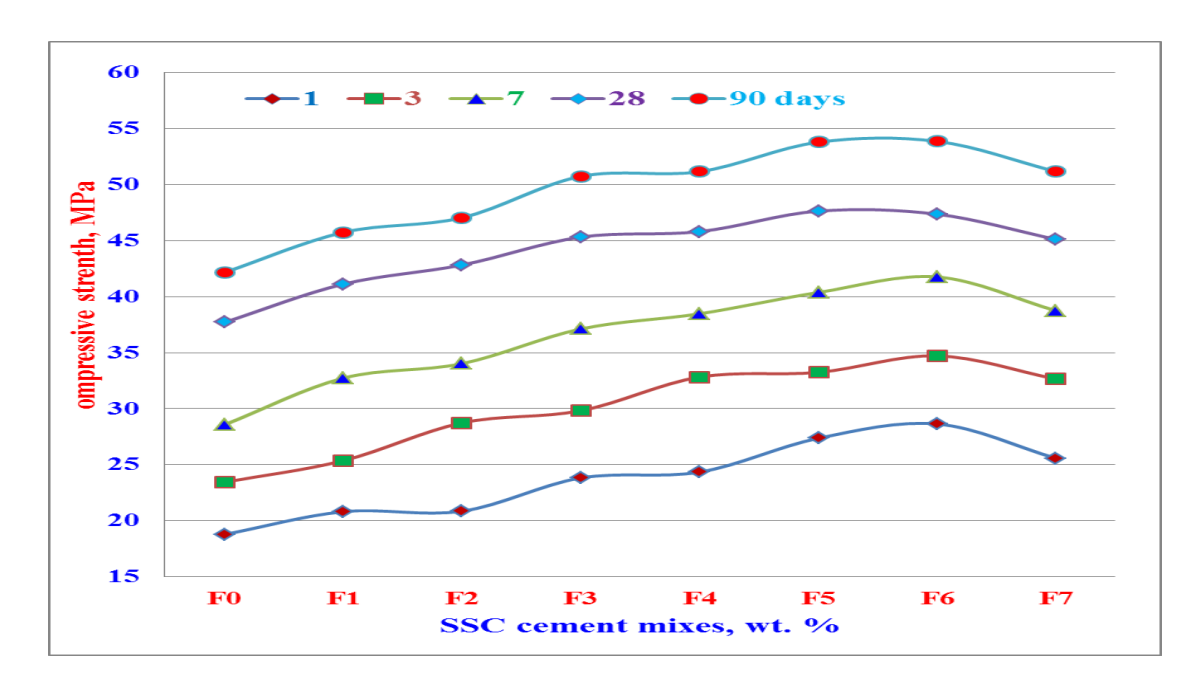


Fig. 8. Compressive strength of SSC cement pastes mixes with different ratios of CF activator and hydrated up to 90 days.

Combined water content

Figure 9 indicates the results of combined water contents of the various SSC pastes blended with CF activator (F0-F7) hydrated as a function of curing times up to 90 days. The combined water content of the control SSC cement (F0) was gradually increased with curing time up to 90 days. The same trend was displayed by all SSC mixes blended with CF (F1-F6). As the CF content increased, the combined water content was increased too. This is essentially contributed to that the CF activated and accelerated the hydration of the different phases of slag, and moreover it may modify the resulting hydration products [39,40], i.e. the CF was so improved the hydration that it could be accelerated the rate of hydration reactions of SSC cement. At early stages of hydration (1-7 days), the combined water content slightly increased, but on 28 up to 90 days, it hardly developed and sharply increased [17,41-43]. The SSC blank (F0) achieved the lowest combined water content, whereas F6 recorded the highest combined water content at 90 days. Blending the SSC with CF > 3%, the combined water content was sharply declined. This is essentially attributed to that the higher alkaline activator content reflected negatively in all characteristics of the SSC cement [45-47]. Consequently, the high content of CF > 3 % must be prevented.

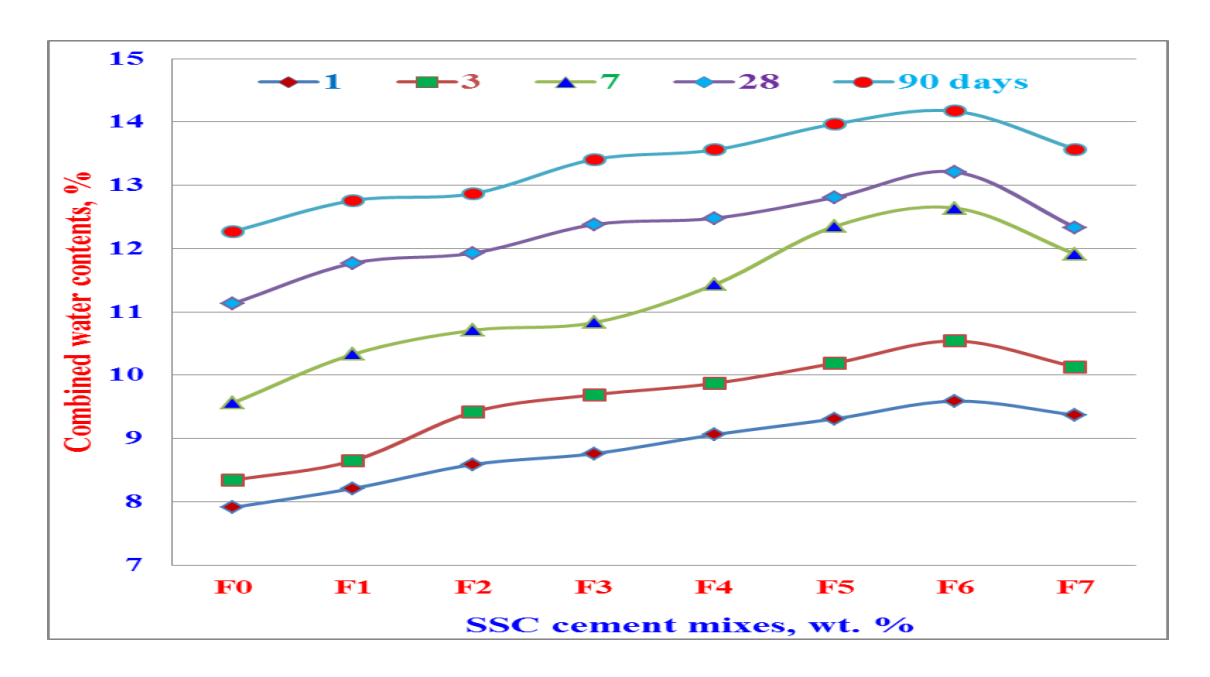


Fig. 9. Combined water contents of SSC cement pastes mixes with different ratios of CF activator and hydrated up to 90 days.

Combined slag and sulfate

The combined slag and sulfate contents of the various SSC pastes blended with CF activator (F0-F7) hydrated as a function of curing times up to 90 days are shown in Figs. 10 and 11, respectively. The combined slag and sulfate in the SSC mixes were determined by the difference between the initial amount of slag or sulfate in the dry cement mix and the free amounts of slag at the end of the prescribed curing time. As the curing time proceeded, both combined slag and sulfate contents increased. The same trend was displayed with all SSC mixes up till 3 wt. % CF activator (F6) and then decreased with any further increase of CF (F7). The slight increase of the reacted or combined slag and sulfate at early ages is mainly due to the formation of ettringite by the consumption of small amount of SO₃. The continuous increase of slag or sulfate consumption with curing time is essentially attributed to the formation of tobermorite-like gel or C-S-H [32,47-51]. The decreased of combined slag or sulfate was caused by the larger amount of CF which was stopped as an obstacle to hydrate normally [52-56]. So, the high content of CF activator must be avoided.

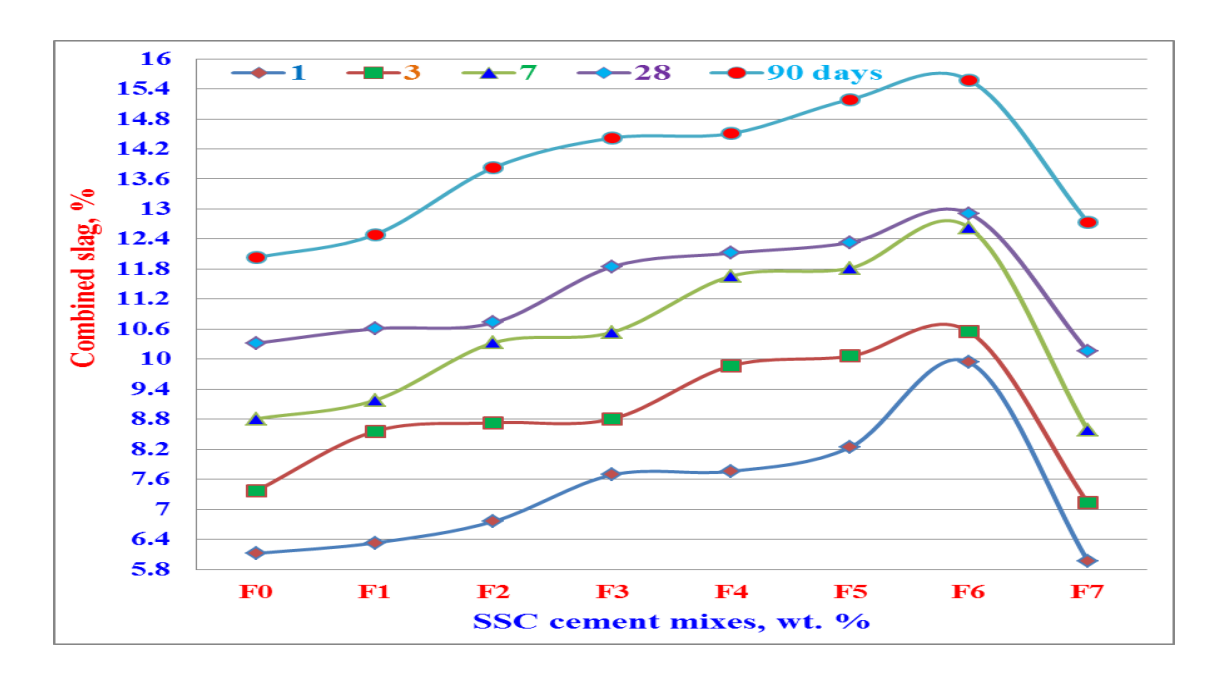


Fig. 10. Combined slag contents of SSC cement pastes mixes with different ratios of CF activator and hydrated up to 90 days.

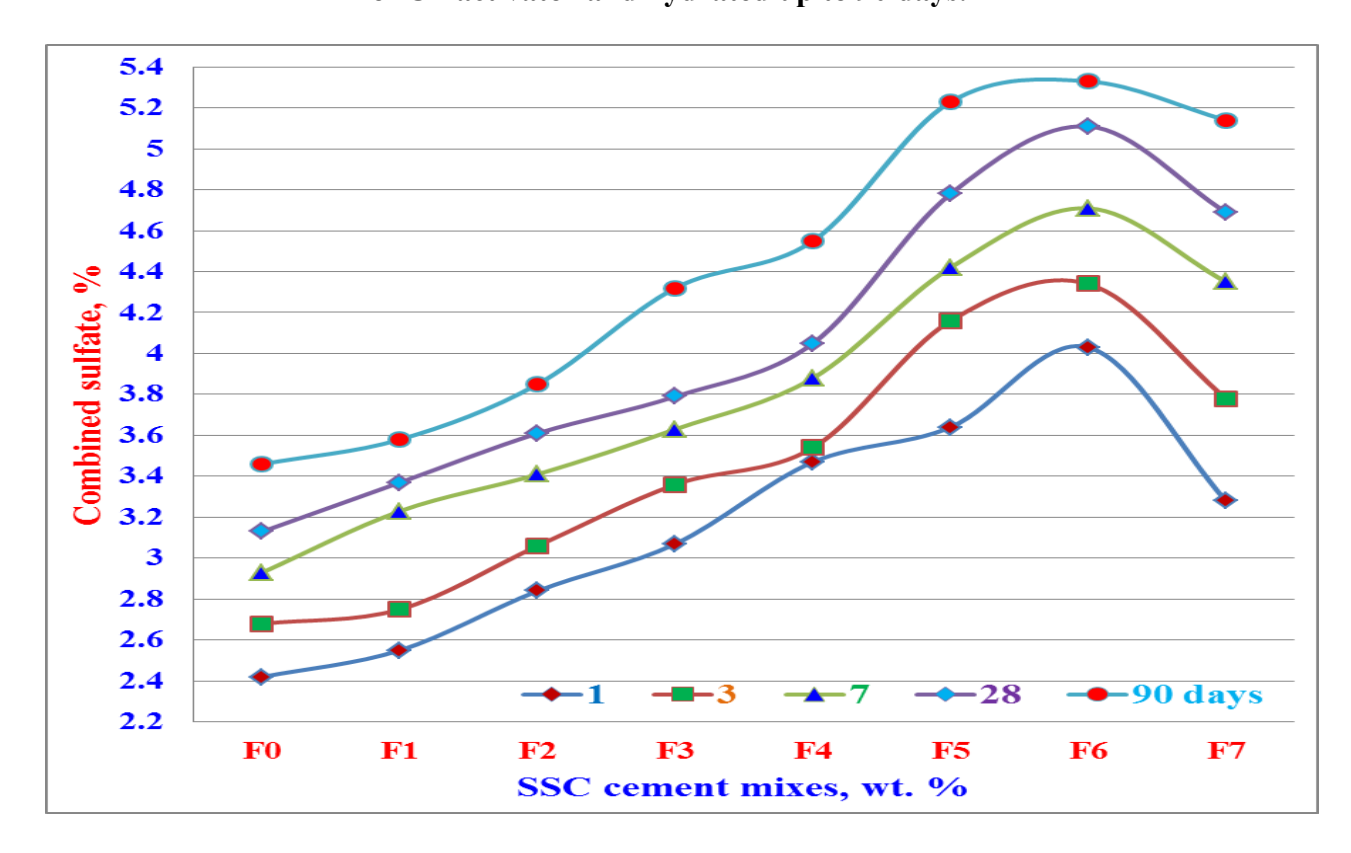


Fig. 11. Combined sulfate contents of SSC cement pastes mixes with different ratios of CF activator and hydrated up to 90 days.

Conclusion

As the early strength of SSC cement is too low, different dosages of CF activator (0, 0.5, 1, 1.5, 2, 2.5, 3 and 3.5 wt. %) were added to activate, accelerate and increase the early hydration process. At early stages of hydration, the CF significantly increases and accelerates the hydration process of the SSC. The water of consistency as well as setting times (Initial and Final) increased with the increase of CF content. Both water absorption and apparent porosity decreased, while the bulk density improved and enhanced. This could be continued only up till 3 wt. % CF (F6), and then these propertied were adversely affected with further increase of CF content (F7). The same trend was displayed with the mechanical properties. Also, the combined water contents exactly followed the other test results. So, CF could improve and promote the hydration of both PC and slag due to the dissolution of both slag and gypsum, which in turn increases the hydration degree of slag. This may be due to that the most Al₂O₃ from the dissolution of the slag was reacted with gypsum to form C-A-S-H hydrates. The reacted or combined slag or sulfate increased with curing time. The crystal-gel ratio plays a vital role in the mechanical strength of SSC cement. Consequently, the cement mix incorporating 3 wt. % of the CF (F6) is the most pronounced effect.

Acknowledgement

This work was supported by National Research Centre, Cairo, Egypt.

Declaration of competing interest

The authors declare that there are no financial or competing conflicts of interest in this work.

Funding

This research article is self-sponsored.

References

- [1] Y. Geng, Z. Wang, L. Shen, and J. Zhao (2019) Calculating of CO₂ emission factors for Chinese cement 463 production based on inorganic carbon and organic carbon, Journal of Cleaner Production, vol. 464 217, 503-509. https://doi.org/10.1016/j.jclepro.2019.01.224.
- [2] M. Shahbaz, D. Balsalobre-Lorente, and A. Sinha (2019) Foreign direct Investment–CO2 emissions 471 nexus in Middle East and North African countries: Importance of biomass energy consumption," 472 Journal of Cleaner Production, 217, 603-614. https://doi.org/10.1016/j.jclepro.2019.01.282.
- [3] L. Wang, L. Chen, J. L. Provis, D. C. W. Tsang, and C. S. Poon (2020) Accelerated carbonation of 466 reactive MgO and Portland cement blends under flowing CO₂ gas, Cement and Concrete Composites, 106. https://doi.org/10.1016/j.cemconcomp.2019.103489.

- [4] D. Coffetti, E. Crotti, G. Gazzaniga, M. Carrara, T. Pastore, and L. Coppola (2022) Pathways towards sustainable concrete, Cement and Concrete Research, 154. https://doi.org/10.1016/j.cemconres.2022.106718.
- [5] Amran M., Makul N., Fediuk R., Lee Y. H., Vatin N. I., Lee Y. Y., Mohammed K. (2022) Global carbon recoverability experiences from the cement industry. Case Studies in Construction Materials, 17, e01439. doi:10.1016/j. cscm.2022.e01439.
- [6] Andrew R. M. (2018) Global CO₂ emissions from cement production, 1928–2017. Earth System Science Data, 10(4), 2213-2239. doi:10.5194/essd-10-2213-2018.
- [7] Potgieter J. H. (2012) An Overview of Cement production: How "green" and sustainable is the industry? Environmental Management and Sustainable Development, 1(2), 14-37. doi:10.5296/emsd.v1i2.1872.
- [8] Sousa V., Bogas J. A. (2021) Comparison of energy consumption and carbon emissions from clinker and recycled cement production. Journal of Cleaner Production, 306, 127277. doi:10.1016/j.jclepro.2021.127277.
- [9] Sun H., Qian J., Yang Y., Fan C., Yue Y. (2020) Optimization of gypsum and slag contents in blended cement containing slag. Cement and Concrete Composites, 112, 103674. doi:10.1016/j.cemconcomp.2020.103674.
- [10] Matschei T., Bellmann F., Stark J. (2005) Hydration behaviour of sulphate-activated slag cements. Advances in Cement Research, 17, 167-178. doi:10.1680/adcr.2005.17.4.167.
- [11] Lu Y., Li S., Tian Y., Meng Y., Chen H., Shi W. (2020) The effect of alkali activator on the properties of super sulfate cement and concrete. Fly Ash Comprehensive Utilization, 34(6), 59-63+115. doi:10.3969/j.issn.1005-8249.2020.06.013.
- [12] Wang J., Yu B. Y., Gao Y. (2014) Hydration characteristics of super sulphated cement with different fineness. 1-4. doi:10.2991/icmaee-14.2014.35.
- [13] Masoudi R., Hooton R. D. (2019) Examining the hydration mechanism of supersulfated cements made with high and low-alumina slags. Cement and Concrete Composites, 103, 193-203. https://doi.org/10.1016/j.cemconcomp.2019.05.001.
- [14] Ren G., Tian Z., Wu J., Gao X. (2021) Effects of combined accelerating admixtures on mechanical strength and microstructure of cement mortar. Construction and Building Materials, 304, 124642. https://doi.org/10.1016/j.conbuildmat.2021.124642.
- [15] Hemalatha T., Sasmal S. (2019) Early-age strength development in fly ash blended cement composites: investigation through chemical activation. Magazine of Concrete Research, 71(5), 260-270. https://doi.org/10.1680/jmacr.17.0033.

- [16] Heikal M. (2004) Effect of calcium format as an accelerator on the physicochemical and mechanical properties of pozzolanic cement pastes. Cement and Concrete Research, 34(6), 1051-1056.
- https://doi.org/10.1016/j.cemconres.2003.11.015.
- [17] Wang Y., Jia J., Cao Q., Gao X. (2022) Effect of calcium format on the compressive strength, and hydration process of cement composite containing fly ash and slag. Journal Geng C., Chen H., Qu Y., Hou P., Li Q., Cheng X. 224 Ceramics Silikáty 68(2) 216-224 (2024) of Building Engineering, 50, 104133. https://doi.org/10.1016/j.jobe.2022.104133.
- [18] Yum W. S., Suh J.-I., Jeon D., Oh J. E. (2020) Strength enhancement of CaO-activated slag system through addition of calcium formate as a new auxiliary activator. Cement and Concrete Composites, 109, 103572. https://doi.org/10.1016/j.cemconcomp.2020.103572.
- [19] Dalconi M. C., Artioli G., Masciocchi N., Giacobbe C., Castiglioni F., Ferrari G. (2021) The crystal structure of a new calcium aluminate phase containing formate. Cement and Concrete Research, 146, 106490. https://doi.org/10.1016/j.cemconres.2021.106490.
- [20] ASTM C187 (1998). Test method for amount of water required for normal consistency of hydraulic cement paste. American Society for Testing and Materials. https://doi.org/10.1520/c0187-98.
- [21] ASTM C191-21 (2021) Standard test methods for time of setting of Hydraulic cement by Vicat Needle. West Conshohocken, PA, USA: ASTM International; 8-10. https://doi.org/10.1520/c0191-01. www.discoveryjournals.org.
- [22] Darweesh HHM (2021) Extraction of lignin from wastes of sugarcane bagasse and its utilization as an admixture for Portland cement, NanoNEXT 2, 1, 13-27. DOI: https://doi.org/10.34256/nnxt2113.
- [23] ASTM C642-13 (2013) Standard Test Method for Density, Absorption, and Voids in Hardened Concrete, ASTM International, West Conshohocken, PA.
- [24] Darweesh HHM, Abu-El-Naga H (2024) The Performance of Portland Cement Pastes (OPC) Incorporated with Ceramic Sanitary Ware Powder Waste (CSPW) at Ambient Temperature, JOURNAL OF SUSTAINABLE MATERIALS PROCESSING AND MANAGEMENT, Vol. 4 No. 1 (2024) 57-70 https://publisher.uthm.edu.my/ojs/index.php/jsmpm.
- [25] Darweesh, H. H. M. (2021) Characterization of coir pith ash blended cement pastes. Research & Development in Material science, RDMS, 851(15), 1630-1639. https://doi.org/10.31031/RDMS.2021.15.000851.
- [26] HHM Darweesh and H Abu-El-Naga (2024) Effect of curing temperatures on the hydration of cement pastes containing nanograin size particles of sanitary ware ceramic powder waste,

- International Journal of Materials Science, 5, 1 07-14. https://www.mechanicaljournals.com/materials-science.
- [27] Darweesh HHM (2024) Reactive magnesia Portland blended cement pastes HHM, Journal of Civil Engineering and Applications, 5, 1, 23-32. http://www.civilengineeringjournals.com/jcea.
- [28] ASTM C348-21 (2021) Standard Test Method for Flexural Strength of Hydraulic-Cement Mortars, ASTM International, West Conshohocken, PA.
- [29] ASTM C109-20 (2020) Standard Test Method for Compressive Strength of Hydraulic Cement Mortars, ASTM International, West Conshohocken, PA. https://doi.org/10.1520/c0109 c0109m-07 527.
- [30] Darweesh HHM (2023) Effect of banana leaf ash as a sustainable material on the hydration of Portland cement pastes, International Journal of Materials Science, 4, 1, 01-11. http://www.mechanicaljournals.com/materials-science.
- [31] Bellmann F., Stark J. (2009): Activation of blast furnace slag by a new method. Cement and Concrete Research, 39 (8), 644-650. https://doi.org/10.1016/j.cemconres.2009.05.012.
- [32] Darweesh HHM, Abu-El-Naga H (2024) The Performance of Portland Cement Pastes (OPC) Incorporated with Ceramic Sanitary Ware Powder Waste (CSPW) at Ambient Temperature, J. of Sustainable Materials Processing and Management Vol. 4, 1, 56-70. https://publisher.uthm.edu.my/ojs/index.php/jsmpm.
- [33] Zhang Q, Liu B, Wang S, Lu X, Li Q, Liu J, Wei S, Fan J, Zhang S (2024) Effect of wet milling activation on mechanical properties and hydration process of cement composites with blast furnace slag, Constr. Build. Mater., 427, 136298. https://doi.org/10.1016/j.conbuildmat.2024.136298.
- [34] Lu X, Liu B, Zhang Q, Wang S, Liu J, Li Q, Fan J, Wei S (2024) Mechanical properties and hydration of fly ash-based geopolymers modified by copper slag, Materials Today Communications 39 (2024) 108914. https://doi.org/10.1016/j.mtcomm.2024.108914.
- [35] Darweesh, HHM (2017). Geopolymer cements from slag, fly ash and silica fume activated with sodium hydroxide and water glass. Interceram-International Ceramic Review, 66(6), 226-231.
- [36] Shen J, Li Y, Lin H, Li H, Lv J, Feng S, Ci J (2022) Prediction of compressive strength of alkali activated construction demolition waste geopolymers using ensemble machine learning, Constr. Build, Mater., 360, 129600. https://doi.org/10.1016/j.conbuildmat.2022.129600.
- [37] Liu SH, Li QL, Han WW (2018) Effect of various alkalis on hydration properties of alkaliactivated slag cements, J. Therm. Anal. Calorim. 131, 3, 3093–3104. https://doi.org/10.1007/s10973-017-6789-z

- [38] Li B, Li Q, Chen W (2021) Spatial zonation of a hydrotalcite-like phase in the inner product of slag: New insights into the hydration mechanism. Cem. Concr. Res., 145, 106460. https://doi.org/10.1016/j.cemconres.2021.106460.
- [39] Lu Y., Li S., Tian Y., Meng Y., Chen H., Shi W. (2020) The effect of alkali activator on the properties of super sulfate cement and concrete. Fly Ash Comprehensive Utilization, 34(6), 59-63+115. https://doi.org/10.1088/1475-7516/2020/06/013.
- [40] Cai T., Hou P., Chen H., Zhao P., Du P., Wang S., Zhou X., Wang X., Cheng X. (2023) Effects of nanosilica on supersulfated cements of different clinker-activation degree. Construction and Building Materials, 365, 130118. https://doi.org/10.1016/j.conbuildmat.2022.130118.
- [41] Masoudi R, Hooton RD (2020) Influence of alkali lactates on hydration of supersulfated cement. Construction and Building Materials, 239, 117844. https://doi.org/10.1016/j.conbuildmat.2019.117844.
- [42] Zhou Y, Peng Z, Chen L, Huang J, Ma T (2021) The influence of two types of alkali activators on the microstructure and performance of supersulfated cement concrete: mitigating the strength and carbonation resistance. Cement and Concrete Composites, 118, 103947. https://doi.org/10.1016/j.cemconcomp.2021.103947.
- [43] Xing J, Zhou Y, Peng Z, Wang J, Jin Y, Jin M (2023) The influence of different kinds of weak acid salts on the macroperformance, micro-structure, and hydration mechanism of the supersulfated cement. Journal of Building Engineering, 66, 105937. https://doi.org/10.1016/j.jobe.2023.105937.
- [44] Zhang Y, Wan Z, de Lima Junior L M, Çopuroğlu O (2022) Early age hydration of model slag cement: Interaction among C3S, gypsum and slag with different Al2O3 contents. Cement and Concrete Research, 161, 106954. https://doi.org/10.1016/j.cemconres.2022.106954.
- [45] Chen H., Hou P., Zhou X., Black L., Adu-Amankwah S., Feng P., Cui N., Glinicki M. A., Cai Y., Zhang S., Zhao P., Li Q., Cheng X. (2023) Toward performance improvement of supersulfated cement by nano silica: Asynchronous regulation on the hydration kinetics of silicate and aluminate. Cement and Concrete Research, 167, 107117. https://doi.org/10.1016/j.cemconres.2023.107117.
- [46] Moula S, A. Fraj AB, Wattez T, Bouasker M, Ali NBH (2023) Mechanical properties, carbon footprint and cost of ultra-high performance concrete containing ground granulated blast furnace slag, J. Build. Eng. 79. https://doi.org/10.1016/j.jobe.2023.107796.
- [47] Zhang Q, Liu B, Wang S, Lu X, Li Q, Liu J, Wei S, Fan J, Zhang S (2024) Effect of wet milling activation on mechanical properties and hydration process of cement composites with blast furnace slag, Constr. Build. Mater., 427, 136298. https://doi.org/10.1016/j.conbuildmat.2024.136298.

- [48] Sharma, R.D., Singh, N. (2023) Evaluation of strength and absorption behaviour of iron slag and recycled aggregates concrete and its comparative environmental estimation by life cycle assessment. Clean. Mater. 10, 100210. https://doi.org/10.1016/J. CLEMA.2023.100210.
- [49] Sultana, I., Islam, G.M.S. (2023) Potential use of ladle furnace slag as supplementary cementitious material in concrete. Case Stud. Constr. Mater. e02141. https://doi.org/10.1016/J.CSCM.2023.E02141.
- [50] Fakhri RS, Dawood ET. (2023) Influence of binary blended cement containing slag and limestone powder to produce sustainable mortar. AIP Conf Proc; 2862(1): 020028. https://doi.org/10.1063/5.0171499.
- [51] Sagade A, Fall M. (2024) Study of fresh properties of cemented paste backfill material with ternary cement blends. Construct Build Mater; 411:134287. https://doi.org/10.1016/j.conbuildmat.2023.134287.
- [52] Zhang Y, Çopuroglu O. (2024) Correlation between slag reactivity and cement paste properties: the influence of slag chemistry. J Mater Civ Eng; 36 (3):04023618. https://doi.org/10.1061/JMCEE7.MTENG-16385.
- [53] Darweesh HHM (2021) Physical and Chemo/Mechanical behaviors of fly ash and silica fume belite cement pastes- Part I, NanoNEXT 2, 2, 1-15. https://doi.org/10.34256/nnxt2121.
- [54] Zhao, Y., Gao, J., Xu, Z., Li, S., Luo, X., Chen, G. (2021) Combined effect of slag and clay brick powder on the hydration of blended cement. Construct. Build. Mater. 299, 123996. https://doi.org/10.1016/j.conbuildmat.2021.123996.
- [55] Li D., Qi Q., Liu Q., Zhu J., Bai Z. (2024): Uniaxial tensile study of calcium aluminosilicate hydrate (C-A-S-H): Structure, dynamics and mechanical properties. Materials Today Communications, 38, 107854. https://doi.org/10.1016/j.mtcomm.2023.10785.
- [56] Chen H., Hou P., Zhou X., Black L., Adu-Amankwah S., Feng P., Cui N., Glinicki M. A., Cai Y., Zhang S., Zhao P., Li Q., Cheng X. (2023): Toward performance improvement of supersulfated cement by nano silica: Asynchronous regulation on the hydration kinetics of silicate and aluminate. Cement and Concrete Research, 167, 107117. https://doi.org/10.1016/j.cemconres.2023.107117.